19th Brazilian Congress of Thermal Sciences and Engineering
November 6th–10th, 2022, Bento Gonçalves - RS - Brazil

ENC-2022-0017
REGIMES AND DYNAMICS OF A DROPLET IMPACTING A HEATED WALL BY HIGH-SPEED SHADOWGRAPHY

Arthur V. S. Oliveira
São Carlos School of Engineering, University of São Paulo, São Carlos/SP, Brazil
avs.oliveira@usp.br

Abstract. *Many processes in thermal engineering involve droplets impacting on heated surfaces: in metallurgy, where spray cooling is used to produce steel plates and bars; in nuclear reactors, where a steam-droplets flow is created during a hypothetical loss-of-coolant accident, and these droplets contribute to the cooling of the fuel assembly; in internal combustion engines, where the injected fuel impinges on the cylinder wall and the piston head. The fluid dynamics process during the droplet impact can play an important role, as it can deposit, splash or bounce on the surface, which affects directly the heat dissipated from the heated wall. The droplet contact time is very short, usually lasting a few micro or milliseconds, which requests high-speed imaging to evaluate correctly its dynamics. In this study, droplet dynamics before, during and after impacting a heated wall were evaluated by high-speed shadowgraphy. The effects of the droplet velocity and wall temperature were analyzed; more precisely, tests were performed for three different impact velocities and three different wall temperatures. The impact regime was identified and the evolutions in the droplet spread diameter and contact angle were measured for each experiment. This study is in the context of a FAPESP Young Investigator research project, in which droplet impact heat transfer and spray cooling will be investigated using several optical techniques, including high-speed shadowgraphy as used herein.*

Keywords: *Spray, Heat transfer, Fluid dynamics, Leidenfrost, Boiling*

1. INTRODUCTION

The many studies in the literature on droplets impacting heated wall is easily explained by its numerous applications in thermal engineering, as listed by Liang and Mudawar (2017) in the review paper. Most of these applications involve spray, like metallurgy for steel cooling (Tsukamoto *et al.*, 2020; Labergue *et al.*, 2015) or fuel injection in internal combustion engines (Chausalkar *et al.*, 2021; Panão and Moreira, 2005), or steam-droplet two-phase flow, like during a loss-of-coolant accident in nuclear reactors (Oliveira *et al.*, 2020a; Jin *et al.*, 2018). Because sprays have a stochastic behavior and only averaged parameters can be evaluated when they are used, many researchers try to characterize single droplet impacts on a heated wall before evaluating spray-impingement systems, even though one can raise doubts about the representative quality of these simpler studies because of the lack of droplet interactions (Moreira *et al.*, 2010).

Despite their limitations, single droplets studies are the first step towards a better understanding of liquid-wall interactions. Both fluid dynamics and heat transfer analyses have already provided useful correlations for more complex studies. For example, Biance *et al.* (2006) model for the droplet impact dynamics that fed Gradeck *et al.* (2013) model for the heat dissipated with the impact of a single droplet on a heated wall that, in turn, was used to estimate the heat dissipation of an internal steam-droplets flow in the Leidenfrost regime by Oliveira *et al.* (2020b). Nevertheless, future studies must start concentrating on evaluating multiple droplet impact processes to understand how droplet interactions affect the heat dissipation in spray cooling. We have examples of investigations that made interesting observations towards a better understanding of droplet interaction effects (Gultekin *et al.*, 2021; Gholijani *et al.*, 2020; Castrejón-Pita *et al.*, 2013), but only with advanced optical techniques we may have important advances to develop mechanistic models for spray cooling, which was already recognized by Kim (2007) in his state-of-the-art review fifteen years ago.

With this motivation, it is undergoing at the São Carlos School of Engineering at the University of São Paulo a research project about the fluid dynamics and heat transfer during the droplet impact onto heated walls, that look to perform experiments with single droplets, multiple droplets and sprays. In this research project, different optical techniques will be used, among them high-speed Shadowgraphy for the measurement of the droplet shape, size and velocity. In the present study, the first steps using this technique are presented to characterize single-droplet impacts on a wall at different temperatures. Three impact velocities and three wall temperatures were tested, and the impact regimes and droplet spread

diameter were evaluated at each condition.

2. EXPERIMENTAL APPARATUS, TEST CONDITIONS AND METHODOLOGY

Figure 1 presents a schematic drawing of the experimental apparatus used in this study. It consists basically of back-light high-speed imaging, also known as Shadowgraphy. A LED light source was used with a diffuser aiming directly at a high-speed camera (Phantom v2012), which worked at 4,000 fps (integration time: 50 μs, pixel size of 28.35 μm). Between the light and the camera, a droplet of tap water was released over an aluminum block using a 34G-gauge needle and a glass syringe. This system provided a very repetitive droplet diameter: about 1.73 mm, varying between 1.72 and 1.75 mm. The aluminum block, the test section, was placed over a heated plate with temperature control. A type-K thermocouple was used to measure the block temperature – which was assumed to be approximately the same temperature as the impacted surface.

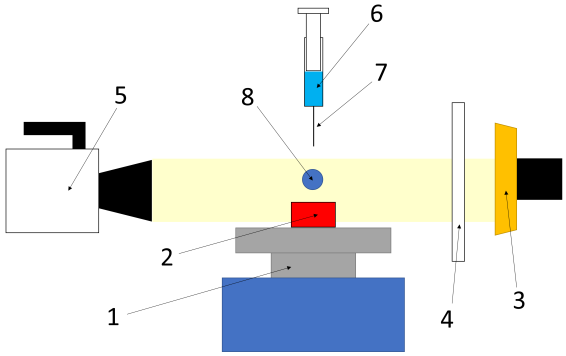

Figure 1. Experimental apparatus for high-speed shadowgraphy: 1) temperature-controlled heating plate; 2) aluminum block (test section); 3) LED light source; 4) light diffuser; 5) high-speed camera; 6) glass syringe; 7) needle; 8) droplet.

Two parameters were varied in these experiments: the droplet height (5, 62 and 164 mm – approximate values), which result in impact velocities from 160 to 1725 mm/s, and the block temperature (22, 140 and 260 °C). Therefore, different impact dynamics could be observed, both because of the droplet kinetic energy at impact and the heat transfer regime (isothermal deposition, nucleate boiling, and Leidenfrost regime). Table 1 summarizes the droplet characteristics for all the tests, like droplet diameter and velocity, and the main non-dimensional numbers that are helpful to evaluate the droplet impact regime – they are presented in the next section.

Table 1. Ranges of the droplet diameter and velocity at impact, as well as its main non-dimensional numbers, for each release height.

h [mm]$^{(1)}$	D_0 [mm]	V_0 [mm/s]	Re_D [-]	We_D [-]
5	1,72 - 1,75	160 - 301	310 - 590	0,61 - 2,2
62	1,73 - 1,74	1058 - 1088	2060 - 2110	27 - 28
164	1,72 - 1,75	1721 - 1725	3320 - 3380	71 - 72

$^{(1)}$ Approximate values, hence the large variation in the impact velocity V_0 for the shortest h.

The test steps were the following. First, the heated plate temperature was set to the desired value – for tests at 22 °C, which were the first to be performed, the heated plate was turned off. Then, using a post holder, the needle height was fixed away from the heated plate to avoid pre-heating of the liquid. After having prepared the camera for recording, the syringe was positioned over the surface, the video recording was started, and the droplet was released. Next, the images were stored, the syringe was re-positioned to the next height, and the next test and recording were performed. These steps were repeated until performing the test at the last height, so the heated plate temperature was increased to the next desired value and all the tests were performed again with the same steps for each height. Finally, after having performed all the experiments for all the plate temperatures, the images were collected and processed and data were extracted as explained in the next section.

3. IMAGE PROCESSING AND DATA REDUCTION

These are the image processing steps used in the present study – Fig. 2 presents some of these steps:

1. All the video frames were collected in grayscale (Fig. 2a) and processed using Matlab. The background was identified with the first 10 frames of a given test and removed in all the images for the same test (Fig. 2b).

2. The impacted surface was identified using the background image by the strong gradient of the gray level at the bottom. Hence, for a vertical line of the image, the pixel corresponding to the surface location can be found using the intensity difference compared to neighbors' values. After sweeping these searches in the horizontal direction for each vertical line, the impacted surface position was found by averaging these pixels' positions. With that information, the instant when the droplet impacted the surface ($t = t_0 = 0$) could be determined.

3. After the droplet impact, the contact angle θ on both sides and the droplet spread diameter D_s were measured for each frame (Fig. 2c). At this step, the image was completely binarized, and D_s was found by detecting the height where the distance between the left and the right borders was the largest. In turn, the contact angle was found by fitting a 4$^{\text{th}}$-order polynomial on the first pixels near the surface and taking the derivative at the surface location. The slope gave the contact angle (Fig. 2d) for each side, and the average was taken for the results presentation of the contact angle. Therefore, it was possible to evaluate the evolution in the spread diameter and contact angle during the droplet impact.

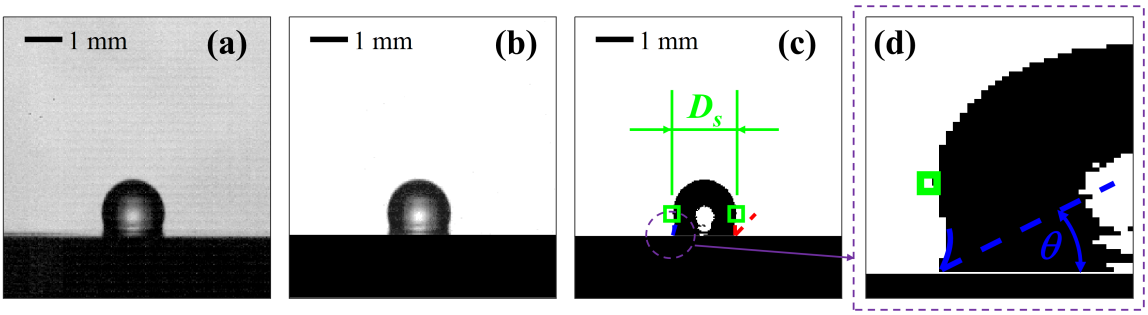

Figure 2. Image processing steps and measurement of the droplet diameter and contact angle: a) raw image; b) image after background removal; c) binary image for the measurement of the droplet diameter D (or spread diameter D_s) with the two extreme pixels found in the droplet (green squares) and contact angle on both sides; d) zoom showing the polynomial fit on one border (filled line) and its slope at origin (dashed line) to calculate the contact angle θ.

The droplet diameter (before impact) and impact velocity were found during the fall of the droplet. Using about 60 frames before the impact, the droplet shape was identified using the Circular Hough Transform (CHT) (*imfindcircles* command in Matlab), which also gave the droplet diameter and centroid position for each frame. Thus, the droplet diameter D_0 was obtained by averaging the measured diameters for the 60 frames, while the droplet impact velocity V_0 was found by fitting a 2$^{\text{nd}}$-order polynomial of the droplet centroid position with time (Fig. 3) and taking its derivative at the impact instant t_0. These values are presented in Table 1.

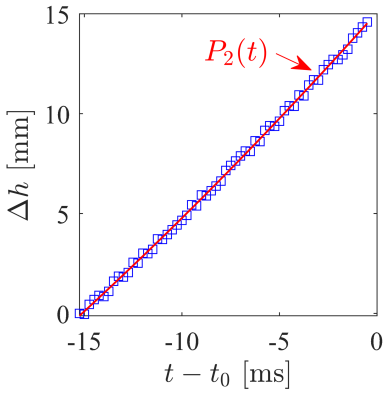

Figure 3. Evolution in the difference between the droplet position at time t – using the impact time t_0 and reference – and the droplet position when first observed in the images. Markers are data points collected from the video and the red line is a second-order polynomial fit with time.

The main non-dimensional numbers used in droplet impact studies are: the Reynolds number Re_D, which is the ratio

of the inertial to viscous forces in the droplet and is defined by:

$$Re_D = \frac{V_0 D_0}{\nu} \tag{1}$$

where ν is the fluid kinematic viscosity; and the Weber number We_D, which is the ratio of the inertial and surface tension forces and given by:

$$We_D = \frac{\rho V_0^2 D_0}{\sigma} \tag{2}$$

where ρ and σ are, respectively, the fluid specific mass and surface tension.

4. RESULTS AND DISCUSSIONS

Images of the droplet impact for wall temperatures T_w at 22, 140 and 260 °C are presented for different Weber numbers in Fig. 4, 6 and 7, respectively. Unfortunately, the images for T_w = 140 °C and We_D = 70 were corrupted during data extraction, so these test results cannot be presented. For T_w = 22 °C (Fig. 4), the droplet adheres completely to the wall after impact for all the Weber numbers, which is characteristic of the deposition regime. It complies with Mundo *et al.* (1995) results, who noted that droplet splashing in these test condition would only occur for Re_D >3000-3500 – hence, the test for We_D = 70 (Re_D = 3300) was near the splashing impact regime. Once the droplet impacts the surface, it spreads over the surface and shrinks back. The spread diameter is higher for higher Weber numbers. Then, its shape oscillates back and forth, increasing and decreasing its spread diameter, until this energy is dissipated and the droplet shape and contact angle reach stability. These observations are clearly made with the results presented in Fig. 5a, where the evolution in the spread diameter (normalized with the initial droplet diameter) and contact angle is presented. After the peak in the spread diameter, it oscillates at a frequency of approximately 200 Hz until reaching a stable shape. This stable droplet spread diameter slightly increases with the increase in the Weber number, possibly because of the larger area of the solid that is wetted by the liquid after spreading, allowing adhesion forces to overcome part of the cohesion forces and stabilizing with a larger solid-liquid contact area. The contact angle follows a similar trend for all We_D and stabilizes nearly at the same value (about 90°).

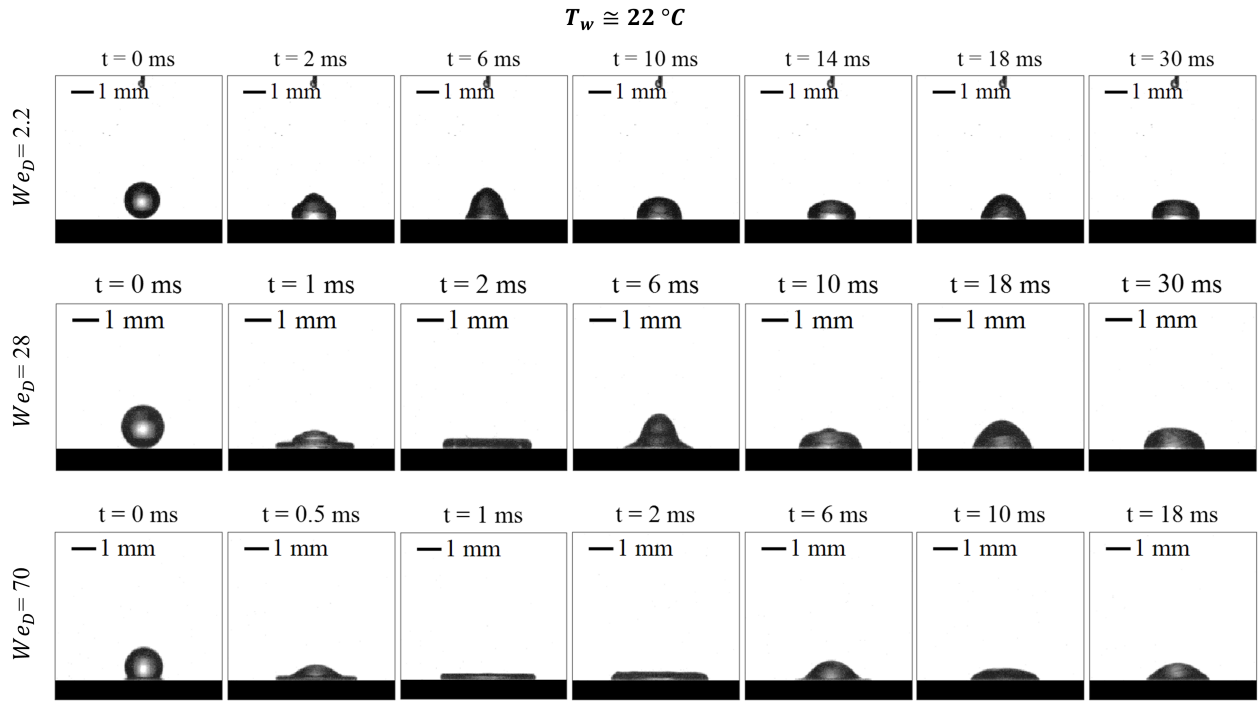

Figure 4. Shadowgraphy images of the droplet impacting on the wall at T_w = 22 °C for different impact velocities (presented as the Weber number We_D. In these conditions, the deposition regime was observed.

When the wall temperature is 140 °C, phase change takes place and the droplet behavior after impact is different from the unheated impact condition(Fig.6), although the impact regime for We_D = 0.61 can be considered deposition. As the wall temperature is sufficiently higher than the fluid saturation temperature, boiling takes place, which was observed

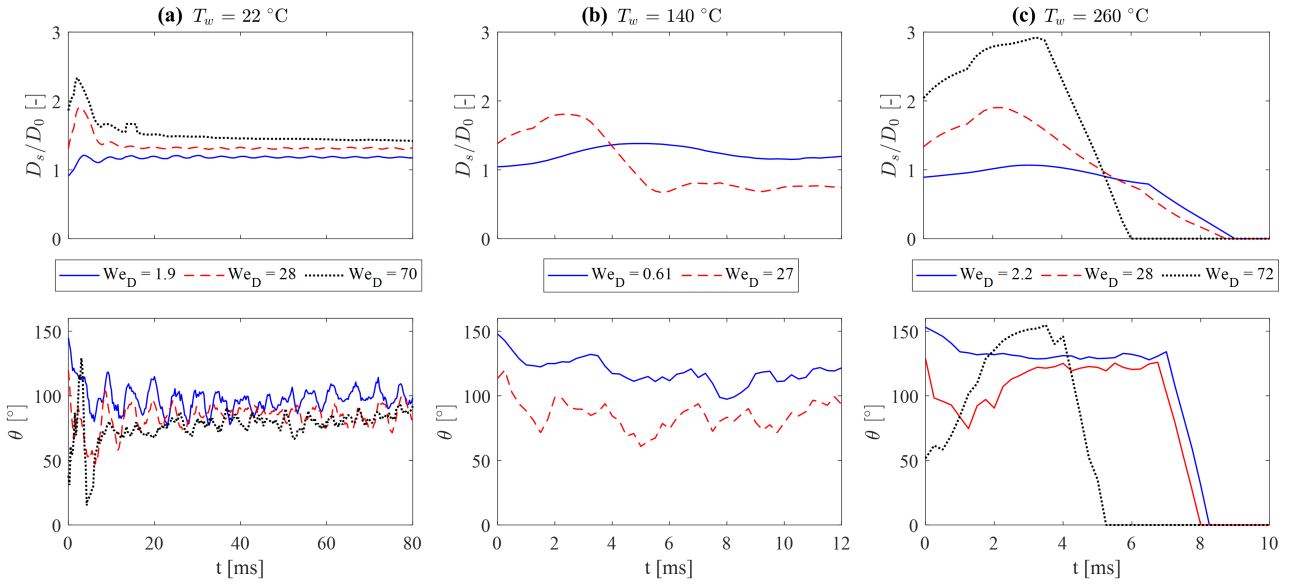

Figure 5. Evolution in the droplet spread diameter and contact angle for each test condition: a) T_w = 22 °C; b) T_w = 140 °C; and c) T_w = 260 °C.

by the bubble formation inside the droplet. Spattering occurred when these bubbles reached the droplet's upper surface, forming tiny droplets. Because of that, the droplet's shape is unstable, looking like it is "dancing", the same observed by Roisman *et al.* (2018) in the transition boiling regime. For this reason, the evolution in D_s and θ for this experiment is only presented for the first milliseconds after the impact (Fig. 5b). Similar to the previous result, the spread diameter is larger for a higher Weber number.

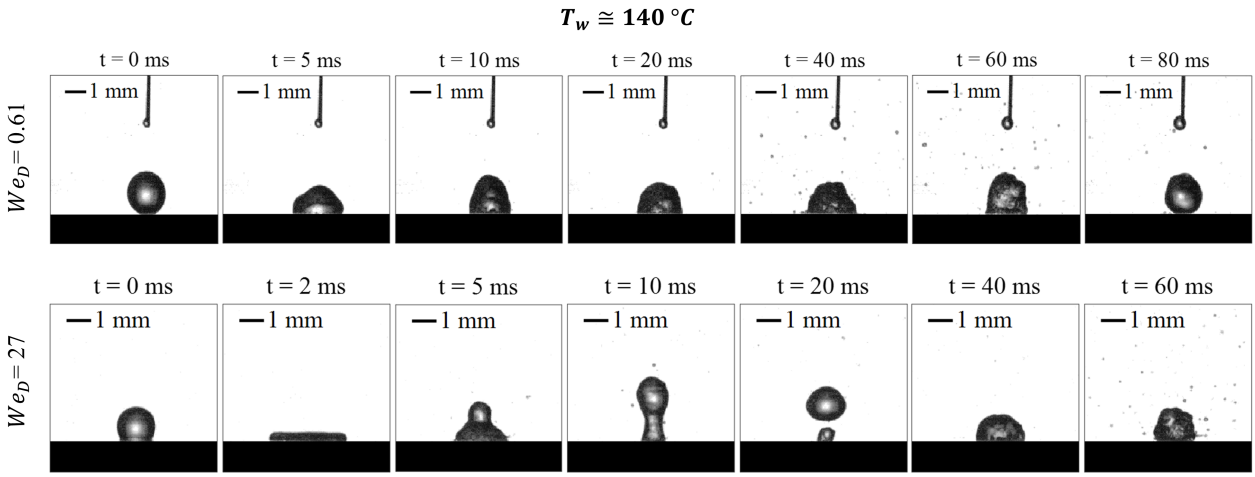

Figure 6. Shadowgraphy images of the droplet impacting on the wall at T_w = 140 °C for different impact velocities (presented as the Weber number We_D. In these conditions, transition boiling regime was observed.

Finally, for T_w = 260 °C, the droplet impact is typical of the Leidenfrost regime, in which the droplet bounces after impact (Fig. 7). For the two lowest Weber numbers, the droplet hits the heated wall, spreads, recoils and bounces off the wall. For We_D = 2.2, it was possible to see the droplet bouncing and impacting the wall several times, at an approximate frequency of 50 Hz. However, for the highest We_D, breakup was observed, which does not comply with the regime map presented by Gradeck *et al.* (2013) (in this condition, the impact regime should be droplet rebound), but complies perfectly with the thermal atomization regime observed by Roisman *et al.* (2018). The droplet rapidly spreads after impact and the spread diameter is much larger than the ones observed in the other experiments – about three times the initial droplet diameter (see Fig. 5c). Therefore, the droplet lamella is very thin at the maximum spreading condition, so it is pierced with the formation of bubbles, forming a rim that recedes very quickly, creating instabilities and, then, breakup. The evidence of the lamella breakup is the spray in fine droplets seen over the spread droplet at t = 2 ms. This phenomenon was both reported by Roisman *et al.* (2018) and Cossali *et al.* (2005).

The maximum droplet spread diameter increases significantly with the increase in the Weber number in the Leidenfrost regime: while the droplet barely spreads for a very flow We_D, the maximum spread diameter doubles for We_D = 28 and triples for We_D = 72. In less than 10 ms, the droplet leaves the surface for all the impact velocities. Concerning the evolution in the contact angle, the droplet spreads as if the surface were hydrophobic, since, in global, $\theta > 90°$. There is an interesting dynamics for the highest We_D that deserves further investigation.

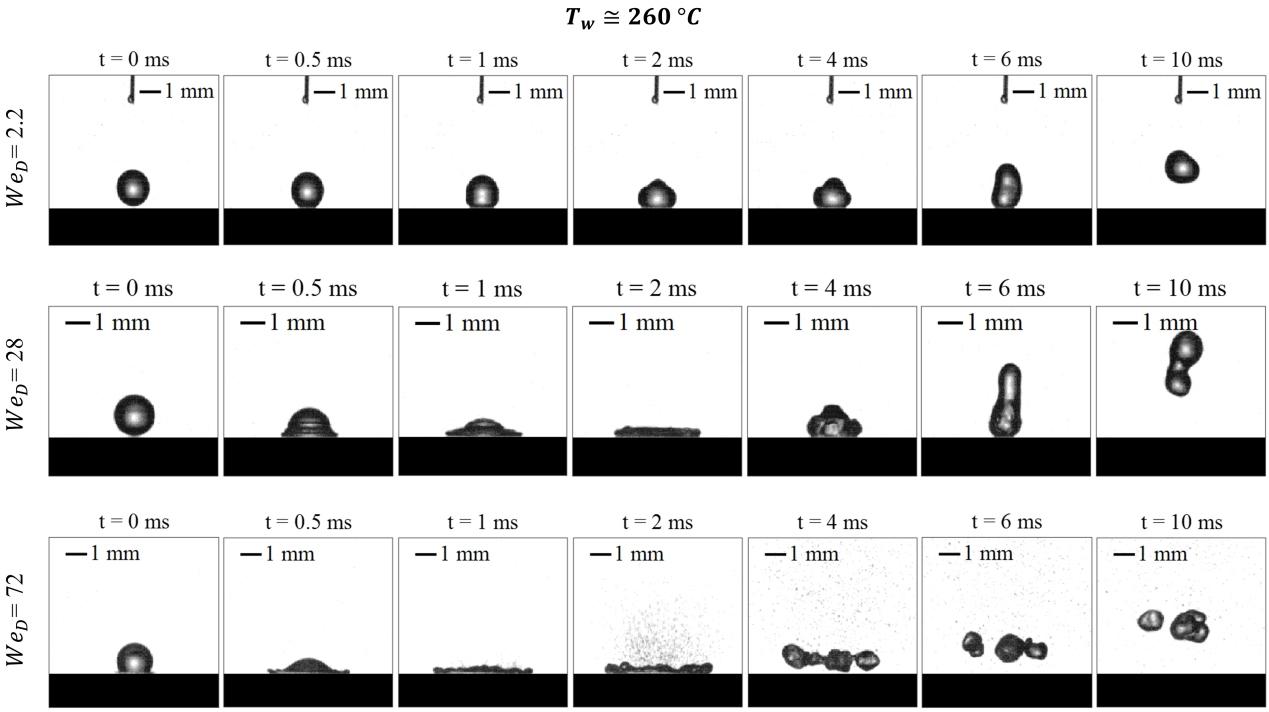

Figure 7. Shadowgraphy images of the droplet impacting on the wall at T_w = 260 °C for different impact velocities (presented as the Weber number We_D. In these conditions, the Leidenfrost regime was observed, as well as the thermal atomization regime for the highest We_D.

5. CONCLUSIONS AND NEXT STEPS

In this study, experimental results using shadowgraphy of droplet impact on a heated surface were presented. Images for different impact velocities and wall temperatures were processed and the results were analyzed. For the unheated condition, only droplet deposition was observed, complying with results published in the literature. Transition boiling was observed for T_w = 140 °C, in which the droplet apparently dances over the surface while spattering forms tiny droplets out of the boiling droplet. In the Leidenfrost regime, rebounding was observed for the two lowest Weber numbers, while thermal atomization was seen for the highest one. In this case, droplet breakup took place because of the breakup of the spreading lamella. The evolution in the droplet spread diameter and contact angle were also presented. In general, the spread diameter increases with the increase in the Weber number.

As mentioned in the introduction, this study is part of a larger study of fluid dynamics and heat transfer of droplets and sprays impacting heated walls. Even though these are the first results, they comply with most of what is available in the literature. Furthermore, these two dynamic results - evolution in the droplet spread diameter and contact angle - provide important information for the modeling of the heat transfer by droplet impact in the Leidenfrost regime. This will be evaluated in the future during this research project with the aid of infrared thermography of the heated surface and laser-induced fluorescence to measure the evolution in the droplet temperature before, during and after impact.

6. ACKNOWLEDGEMENTS

The author gratefully acknowledges São Paulo Research Foundation (FAPESP) for the Young Investigator Research Grant (#2021/01897-0), the scholarship given to the author (#2022/00040-1) and the funding for the high-speed camera as a multiuser equipment (#2019/08577-1).

7. REFERENCES

Biance, A.L., Chevy, F., Clanet, C., Lagubeau, G. and Quéré, D., 2006. "On the elasticity of an inertial liquid shock". *Journal of Fluid Mechanics*, Vol. 554, p. 47–66. doi:https://doi.org/10.1016/10.1017/S0022112006009189.

Castrejón-Pita, J.R., Kubiak, K.J., Castrejón-Pita, A.A., Wilson, M.C.T. and Hutchings, I.M., 2013. "Mixing and internal dynamics of droplets impacting and coalescing on a solid surface". *Phys. Rev. E*, Vol. 88, p. 023023. doi: https://link.aps.org/doi/10.1103/PhysRevE.88.023023.

Chausalkar, A., Kweon, C.B.M. and Michael, J.B., 2021. "Multi-component fuel drop-wall interactions at high ambient pressures". *Fuel*, Vol. 283, p. 119071. ISSN 0016-2361. doi:https://doi.org/10.1016/j.fuel.2020.119071.

Cossali, G., Marengo, M. and Santini, M., 2005. "Secondary atomisation produced by single drop vertical impacts onto heated surfaces". *Experimental Thermal and Fluid Science*, Vol. 29, No. 8, pp. 937–946. ISSN 0894-1777. doi: https://doi.org/10.1016/j.expthermflusci.2004.12.003.

Gholijani, A., Gambaryan-Roisman, T. and Stephan, P., 2020. "Experimental investigation of hydrodynamics and heat transport during vertical coalescence of multiple successive drops impacting a hot wall under saturated vapor atmosphere". *Experimental Thermal and Fluid Science*, Vol. 118, p. 110145. ISSN 0894-1777. doi: https://doi.org/10.1016/j.expthermflusci.2020.110145.

Gradeck, M., Seiler, N., Ruyer, P. and Maillet, D., 2013. "Heat transfer for leidenfrost drops bouncing onto a hot surface". *Experimental Thermal and Fluid Science*, Vol. 47, pp. 14–25. ISSN 0894-1777. doi: https://doi.org/10.1016/j.expthermflusci.2012.10.023.

Gultekin, A., Erkan, N., Ozdemir, E., Colak, U. and Suzuki, S., 2021. "Simultaneous multiple droplet impact and their interactions on a heated surface". *Experimental Thermal and Fluid Science*, Vol. 120, p. 110255. ISSN 0894-1777. doi:https://doi.org/10.1016/j.expthermflusci.2020.110255.

Jin, Y., Cheung, F.B., Bajorek, S.M., Tien, K. and Hoxie, C.L., 2018. "Investigation of the thermal-hydraulic non-equilibrium in a 7x7 rod bundle during reflood". *International Journal of Heat and Mass Transfer*, Vol. 127, pp. 266–279. ISSN 0017-9310. doi:https://doi.org/10.1016/j.ijheatmasstransfer.2018.08.011.

Kim, J., 2007. "Spray cooling heat transfer: The state of the art". *International Journal of Heat and Fluid Flow*, Vol. 28, No. 4, pp. 753–767. ISSN 0142-727X. doi:https://doi.org/10.1016/j.ijheatfluidflow.2006.09.003. Including Special Issue of Conference on Modelling Fluid Flow (CMFF'06), Budapest.

Labergue, A., Gradeck, M. and Lemoine, F., 2015. "Comparative study of the cooling of a hot temperature surface using sprays and liquid jets". *International Journal of Heat and Mass Transfer*, Vol. 81, pp. 889–900. ISSN 0017-9310. doi:https://doi.org/10.1016/j.ijheatmasstransfer.2014.11.018.

Liang, G. and Mudawar, I., 2017. "Review of drop impact on heated walls". *International Journal of Heat and Mass Transfer*, Vol. 106, pp. 103–126. ISSN 0017-9310. doi:https://doi.org/10.1016/j.ijheatmasstransfer.2016.10.031.

Moreira, A., Moita, A. and Panão, M., 2010. "Advances and challenges in explaining fuel spray impingement: How much of single droplet impact research is useful?" *Progress in Energy and Combustion Science*, Vol. 36, No. 5, pp. 554–580. ISSN 0360-1285. doi:https://doi.org/10.1016/j.pecs.2010.01.002.

Mundo, C., Sommerfeld, M. and Tropea, C., 1995. "Droplet-wall collisions: Experimental studies of the deformation and breakup process". *International Journal of Multiphase Flow*, Vol. 21, No. 2, pp. 151–173. ISSN 0301-9322. doi:https://doi.org/10.1016/0301-9322(94)00069-V.

Oliveira, A.V.S., Peña Carrillo, J.D., Labergue, A., Glantz, T. and Gradeck, M., 2020a. "Experimental study of dispersed flow film boiling at sub-channel scale in LOCA conditions: Influence of the steam flow rate and residual power". *Applied Thermal Engineering*, Vol. 172, p. 115143. ISSN 1359-4311. doi: https://doi.org/10.1016/j.applthermaleng.2020.115143.

Oliveira, A.V.S., Peña Carrillo, J., Labergue, A., Glantz, T. and Gradeck, M., 2020b. "Mechanistic modeling of the thermal-hydraulics in polydispersed flow film boiling in LOCA conditions". *Nuclear Engineering and Design*, Vol. 357, p. 110388. ISSN 0029-5493. doi:https://doi.org/10.1016/j.nucengdes.2019.110388.

Panão, M. and Moreira, A., 2005. "Thermo- and fluid dynamics characterization of spray cooling with pulsed sprays". *Experimental Thermal and Fluid Science*, Vol. 30, No. 2, pp. 79–96. ISSN 0894-1777. doi: https://doi.org/10.1016/j.expthermflusci.2005.03.020.

Roisman, I.V., Breitenbach, J. and Tropea, C., 2018. "Thermal atomisation of a liquid drop after impact onto a hot substrate". *Journal of Fluid Mechanics*, Vol. 842, p. 87–101. doi:https://doi.org/10.1017/jfm.2018.123.

Tsukamoto, K., Kita, Y., Inoue, S., Hamanosono, T., Hidaka, S., Ueoka, S., Fukuda, H., Kohno, M. and Takata, Y., 2020. "On the onset of quench during spray cooling: The significance of oxide layers". *Applied Thermal Engineering*, Vol. 179, p. 115682. ISSN 1359-4311. doi:https://doi.org/10.1016/j.applthermaleng.2020.115682.

8. RESPONSIBILITY NOTICE

The author is solely responsible for the printed material included in this paper.